Available online at www.sciencedirect.com
ScienceDirect
Metabolism Clinical and Experimental 60 (2011) 617–628
Metabolism
Clinical and Experimental
www.metabolismjournal.com

Ezetimibe decreases SREBP-1c expression in liver and reverses hepatic insulin resistance in mice fed a high-fat diet

Tomonori Muraoka[a], Kazutaka Aoki[a], Tomoyuki Iwasaki[a], Kazuaki Shinoda[a], Akinobu Nakamura[a], Hiroyuki Aburatani[b], Shuuichi Mori[c], Kumpei Tokuyama[c], Naoto Kubota[d], Takashi Kadowaki[d], Yasuo Terauchi[a,*]

[a]*Department of Endocrinology and Metabolism, Yokohama City University Graduate School of Medicine, Yokohama 236-0004, Japan*
[b]*Genome Science Division, Research Center for Advanced Science and Technology, University of Tokyo, Tokyo 153-8904, Japan*
[c]*Graduate School of Comprehensive Human Sciences, University of Tsukuba, Tsukuba 305-0006, Japan*
[d]*Department of Metabolic Diseases, Graduate School of Medicine, University of Tokyo, Tokyo 113-8655, Japan*

Received 21 December 2009; accepted 7 June 2010

Abstract

Ezetimibe inhibits intestinal cholesterol absorption, thereby reducing serum cholesterol. Recent studies suggest that ezetimibe affects liver steatosis and insulin resistance. We investigated the impact of ezetimibe on insulin sensitivity and glucose metabolism in C57BL/6 mice. We analyzed 4 mouse groups fed the following diets: normal chow (4% fat) for 12 weeks, normal chow for 10 weeks followed by normal chow plus ezetimibe for 2 weeks, high-fat chow (32% fat) for 12 weeks, and high-fat chow for 10 weeks followed by high-fat chow plus ezetimibe for 2 weeks. In the normal chow + ezetimibe group, ezetimibe had no impact on body weight, fat mass, lipid metabolism, liver steatosis, glucose tolerance, or insulin sensitivity. In the high-fat chow + ezetimibe group, ezetimibe had no impact on body weight or fat mass but significantly decreased serum low-density lipoprotein cholesterol, triglyceride, and glutamate pyruvate transaminase levels; liver weight; hepatic triglyceride content; and hepatic cholesterol content and increased the hepatic total bile acid content. In association with increases in IRS-2 and Akt phosphorylation, ezetimibe ameliorated hepatic insulin resistance in the high-fat chow + ezetimibe group, but had no effect on insulin sensitivity in primary cultured hepatocytes. A DNA microarray and Taqman polymerase chain reaction revealed that ezetimibe up-regulated hepatic SREBP2 and SHP expression and down-regulated hepatic SREBP-1c expression. SHP silencing mainly in the liver worsened insulin resistance, and ezetimibe protected against insulin resistance induced by down-regulation of SHP. Ezetimibe down-regulated SREBP-1c in the liver and reversed hepatic insulin resistance in mice fed a high-fat diet.

1. Introduction

Ezetimibe is a novel sterol absorption inhibitor that blocks Niemann-Pick C1-Like 1 (NPC1L1)–mediated cholesterol absorption in the apical brush border membrane of jejunal enterocytes [1]. NPC1L1 null mice were completely resistant to high-cholesterol-diet–induced hypercholesterolemia, with plasma lipoprotein and hepatic cholesterol profiles similar to those of wild-type mice treated with ezetimibe [2]. Ezetimibe prevented lipid-rich-diet–induced increase in biliary cholesterol in hamsters [3]. Recently, potential consequences of ezetimibe relative to metabolism of other nutrients have been investigated. In animal experiments, ezetimibe reversed diet-induced obesity [4,5], liver steatosis [4-7], and insulin resistance [6]. In humans, in addition to the effect of ezetimibe on lowering serum low-density lipoprotein (LDL) cholesterol [8], its potential effects on liver steatosis [9] and insulin resistance [10] have been reported. Nevertheless, the mechanism whereby ezetimibe achieves these favorable effects on insulin sensitivity remains unclear. These circumstances prompted us to investigate the effects of ezetimibe on insulin sensitivity and glucose metabolism using high-fat-diet–induced C57BL/6 obese mice to pursue the possibility of new mechanisms explaining these beneficial effects.

* Corresponding author. Tel.: +81 45 787 2639.
E-mail address: terauchi@yokohama-cu.ac.jp (Y. Terauchi).

0026-0495/$ – see front matter © 2011 Elsevier Inc. All rights reserved.
doi:10.1016/j.metabol.2010.06.008

2. Materials and methods

2.1. Chemicals

Ezetimibe is a novel sterol absorption inhibitor that blocks NPC1L1-mediated cholesterol/phytosterol absorption in the apical brush border membrane of jejunal enterocytes, as described previously [1]. The Schering-Plough Research Institute provided us with ezetimibe.

2.2. Animals and diet protocol

Male C57BL/6 mice (7 weeks of age) (Japan SLC, Shizuoka, Japan) were fed a normal chow diet (Type MF; Oriental Yeast, Tokyo, Japan) for 1 week and were then divided into 4 groups that were each fed a specific diet for the next 12 weeks. We thus analyzed 4 mouse groups, namely, mice fed a normal chow diet for 12 weeks (NC), mice fed a normal chow diet for 10 weeks followed by normal chow diet containing 0.005% wt/wt ezetimibe for 2 weeks (NC + Ez), mice fed a high-fat chow (High-Fat Diet 32; CLEA Japan, Tokyo, Japan) for 12 weeks (HF), and mice fed a high-fat chow for 10 weeks followed by high-fat chow containing 0.005% wt/wt ezetimibe for 2 weeks (HF + Ez). Cholesterol absorption is inhibited by more than 90% at ezetimibe doses of more than 3 mg/kg in apolipoprotein E–knockout mice [11]. The target doses of 0.005% wt/wt ezetimibe mixed in either normal chow or high-fat chow corresponded to a dose of 3 mg/kg body weight in the C57BL/6J mice. The nutrient compositions of the chows are described in Table 1. The mice were given free access to water and food until the start of the experiments. The experiments were approved by the Ethical Committee for Animal Experimentation of Yokohama City Medical University, and the animals were maintained according to standard animal care procedures based on institutional guidelines.

2.3. Measurement of lipids and bile acid

The extraction of lipids from liver tissue was performed as described by Folch et al [12]. Plasma lipoproteins were analyzed using an online dual enzymatic method for the simultaneous quantification of cholesterol and triglycerides (TGs) using high-performance liquid chromatography at Skylight Biotech (Akita, Japan), according to the procedure reported by Usui et al [13]. The total bile acid level in the serum was determined by using enzymatic methods at SRL (Tokyo, Japan). Bile acid in the liver was extracted using the ethanol-thermal method, and the bile acid content was determined using enzymatic methods at Skylight-Biotec according to the procedure reported by Udagawa et al [14] with slight modifications.

Table 1
Nutritional components of Type MF and High-Fat Diet 32

	Type MF	High-Fat Diet 32
Moisture (g/100 g)	7.8	6.9
Content of crude protein (g/100 g)	23.8	25.0
Content of crude fat (g/100 g)	3.7	32.4
Content of crude ash (g/100 g)	6.1	4.0
Content of crude fiber (g/100 g)	3.2	2.9
Nitrogen-free extract (g/100 g)	54.0	28.8
Cholesterol content (mg/100 g)	75	12.9
Calorie (kcal/100 g)	357	507.6

2.4. Histology of the liver

To study the liver histology, the livers were dissected and fixed in buffered neutral formalin (10%). The fixed-tissue blocks were embedded in paraffin, and 4-μm paraffin sections were stained using the standard hematoxylin and eosin staining procedure.

2.5. Oral glucose tolerance test

Each group of mice was given an oral glucose tolerance test (1.5 mg of glucose per gram of body weight after 18 hours of fasting). The glucose levels were measured at 0, 15, 30, 60, and 120 minutes using whole blood obtained from the tail vein and a portable blood glucose analyzer (Glutest Neo; Sanwa Chemical, Nagoya, Japan); the insulin levels were measured at 0, 15, and 30 minutes using an enzyme-linked immunosorbent assay kit (Morinaga, Kanagawa, Japan), as previously described [15].

2.6. Insulin tolerance test

Each group of mice was given an insulin tolerance test. Mice were given free access to food and were then intraperitoneally injected with 0.75 mU of insulin per gram of body weight. The glucose levels were then measured at 0, 15, 30, 60, and 120 minutes using whole blood obtained from the tail vein and a portable blood glucose analyzer (Glutest Neo).

2.7. Hyperinsulinemic-euglycemic clamp study

Clamp studies were performed as described previously [16-18]. Briefly, 2 to 3 days before the study, an infusion catheter was inserted into the right jugular vein under general anesthesia with sodium pentobarbital. Studies were performed on mice under conscious and unstressed conditions after a 6-hour fast. A primed continuous infusion of insulin (Humulin R; Eli Lilly and Company, Indianapolis, IN, USA) was given (5.0 mU/[kg min]), and the blood glucose concentration, monitored every 5 minutes, was maintained at 120 mg/dL through the administration of glucose (5 g of glucose per 10 mL enriched to approximately 20% with [6,6-2H2]glucose [Sigma, Tokyo, Japan]) for 120 minutes. Blood was sampled via tail tip bleeds at 90, 105, and 120 minutes to determine the rate of glucose disappearance (Rd). Rd was calculated using non–steady-state equations, and endogenous glucose production (EGP) was calculated as the difference between Rd and the exogenous glucose infusion rate (GIR).

2.8. In vivo IRS-1/2 and Akt phosphorylation

The monoclonal antiphosphotyrosine antibody (anti-PY), polyclonal anti–IRS-1 antibody (anti–IRS-1), and polyclonal anti–IRS-2 antibody (anti–IRS-2) were purchased from Upstate Biotechnology (Lake Placid, NY, USA). Rabbit polyclonal anti–phospho-Akt antibody (anti-pAkt) recognizing phosphorylated Ser-473 of Akt1 and rabbit anti-Akt antibody (anti-Akt) were purchased from Cell Signaling Technology (Beverly, MA). Mice in the HF and HF + Ez groups were starved for 24 hours, anesthetized with pentobarbital, and injected with 15 units of regular human insulin (Humulin R) or saline into the inferior vena cava. Seventy seconds later, the livers were excised and homogenized in ice cold buffer A (25 mmol/L Tris-HCl [pH 7.4], 10 mmol/L Na_3VO_4, 10 mmol/L NaPPi, 100 mmol/L NaF, 10 mmol/L EDTA, 10 mmol/L EGTA, and 1 mmol/L phenylmethylsulfonyl fluoride). Lysates were prepared by centrifugation (15 000 rpm, 20 minutes, 4°C). Immunoprecipitation analyses for either IRS-1 or IRS-2 and Western blot analyses for Akt and pAkt were then performed. To detect the immunoprecipitation of either IRS-1 or IRS-2 and their phosphorylation, liver extracts were incubated with specific antibodies against either IRS-1 or IRS-2 at 4°C overnight and then with protein G–Sepharose for 2 hours at 4°C. After washing 3 times with buffer A, the immunocomplexes were resolved on 7% sodium dodecyl sulfate polyacrylamide gel electrophoresis. The phosphorylated or total protein was then analyzed using immunoblotting with specific antibodies against either IRS-1 or IRS-2 and a phosphotyrosine antibody. Akt activity was expressed as the ratio of the intensity of pAkt to Akt.

2.9. RNA preparation and microarray analysis of messenger RNA levels in the liver

Mice in the HF and HF + Ez groups were subjected to fasting for 24 hours. Total RNA was prepared from portions of the liver using Isogen Reagent (NipponGene, Tokyo, Japan) according to the manufacturer's instructions. RNA was further purified using a NucleoSpin RNA II column (Macherey-Nagel, Duren, Germany), and RNA quality was assessed after electrophoresis in a 1% agarose gel. GeneChip assays were then performed, as previously described [18]. Briefly, double-strand standard complementary DNA with a T7 promoter was synthesized from 5 μg of total RNA using the SuperScript choice system (Invitrogen-Life Technologies, Carlsbad, CA, USA). Approximately 50 μg of biotin-labeled complementary RNA was synthesized using in vitro transcription with T7 polymerase. After purification and fragmentation, complementary RNA was hybridized to the oligonucleotide microarray (Mouse Genome 430 2.0 Array; Affymetrix, Santa Clara, CA, USA). The scanned images were interpreted using GeneChip Operating Software 1.4 (Affymetrix) to generate a score representing the expression level of each gene. The microarray data have been deposited in the Gene Expression Omnibus public database.

2.10. Taqman polymerase chain reaction

Total RNA was prepared as mentioned above. The messenger RNA levels in the liver were quantitatively analyzed using fluorescence-based reverse transcriptase polymerase chain reaction (PCR). The reverse transcription mixture was amplified using specific primers and an ABI Prism 7500 sequence detector equipped with a thermocycler. The primers were purchased from Applied Biosystems (Foster City, CA). The relative expression levels were compared after normalization to β-actin [19].

2.11. Establishment of primary cultured hepatocytes and in vitro Akt phosphorylation experiment

Mice were anesthetized by the intraperitoneal administration of pentobarbital (40 mg/kg). Mouse hepatocytes were then isolated by the perfusion of collagenase through the abdominal vein, as previously described [20,21]. Briefly, the liver was perfused with a calcium-free Hanks HEPES buffer containing EGTA, followed by perfusion with Hanks HEPES buffer containing collagenase (0.1%). The "softened" liver was then excised, and the hepatocytes were separated from the connective tissue by filtering through macroporous filters (150 mesh; Ikemoto Scientific Technology, Tokyo, Japan). To remove nonparenchymal cells, the hepatocytes were washed with Williams medium E in Hanks buffer by repeated centrifugation for 3 minutes (each time) at 50*g*. The cell pellet was resuspended in Williams medium E containing streptomycin (100 μg/mL), penicillin (100 U/mL), and fetal bovine serum (10%); and the cell suspension was seeded into 24-well collagen-coated plates. The cells were cultured at 37°C under 5% CO_2 humidified air. After overnight incubation, the cells were washed with phosphate-buffered saline (PBS); and the buffer was changed to glucose-free Hanks solution, a substrate for gluconeogenesis, as previously described [22]. The cells were washed with PBS and then treated with ezetimibe (25 μmol/L) or dimethyl sulfoxide in medium for 48 hours, followed by treatment with insulin (10 nmol/L) or PBS for 5 minutes, as previously described [4]. The cells were lysed and subjected to Western blot analysis, as described above. Akt activity was expressed as the ratio of the intensity of pAkt to Akt.

2.12. Preparations of small interfering RNA and small interfering RNA treatment

Synthetic small interfering RNA (siRNA) was purchased from Takara Bio (Shiga, Japan). Sequences of the sense and anti-sense strands of siRNA were 5′-CGGACUUCCUUGCUUUGGATT-3′ and 5′-UCCAAAGCAAGGAACUCGTT-3′, respectively. Synthetic siRNAs were delivered in vivo using a modified hydrodynamic transfection method [23]. Mice fed a high-fat chow for 10 weeks were fasted 12 hours before hydrodynamic injection. Fifty micrograms siRNA dissolved in 2 mL Ringer buffer was rapidly injected into the tail vein, and then mice were immediately refed either

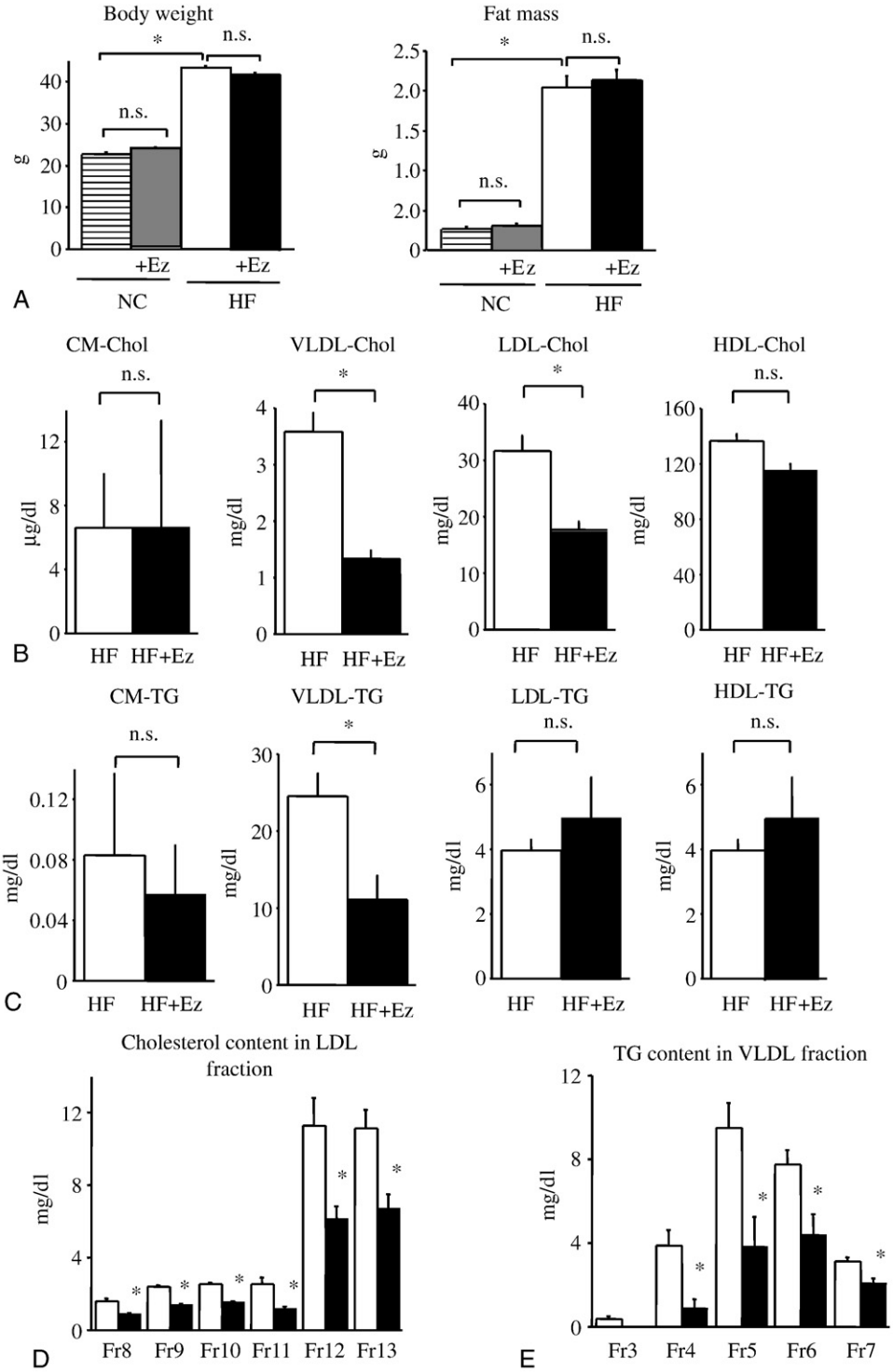

Fig. 1. Impact of ezetimibe on body weight, fat mass, and lipid metabolism in mice fed either a normal chow diet or a high-fat diet. A, Body weight and epididymal fat weight after 12 weeks on either diet. Mice were fed NC (striped bar), NC + Ez (gray bar), HF (open bar), or HF + Ez (filled bar) (n = 9-13). B, Cholesterol content in each lipoprotein in the HF (open bar) and HF + Ez (filled bar) groups (n = 6). The cholesterol contents in chylomicron, VLDL, LDL, and high-density lipoprotein were determined. C, Triglyceride content in each lipoprotein in the HF and HF + Ez groups (n = 6). The TG contents in chylomicron, VLDL, LDL, and high-density lipoprotein were determined. D, Cholesterol content in LDL fraction further analyzed in 6 subfractions according to particle size (n = 6). E, Triglyceride content in VLDL further analyzed in 6 subfractions according to particle size (n = 6). Values are the means ± SE. *$P < .05$. CM indicates chylomicron; HDL, high-density lipoprotein.

high-fat chow or high-fat chow containing 0.005% wt/wt ezetimibe for 2 weeks. Body weight, fat mass, liver weight, and fasting plasma glucose were measured at the indicated time points after injection; and total RNA was prepared. Insulin tolerance test was conducted at the indicated time point: Mice were given free access to food and were then intraperitoneally injected with 1.5 mU of insulin per gram of body weight.

2.13. Statistical analysis

Results were expressed as the means ± SEM. Statistical differences were analyzed using the Student *t* test for unpaired comparisons and Scheffe test for comparisons among the 3 or 4 groups of mice using StatView software, version 5.0 (SAS, Cary, NC). A P value < .05 was considered statistically significant.

3. Results

3.1. No impact of ezetimibe on body weight or fat mass in mice fed a normal chow or high-fat diet

A high-fat diet treatment significantly increased body weight and fat mass, but the 2-week administration of

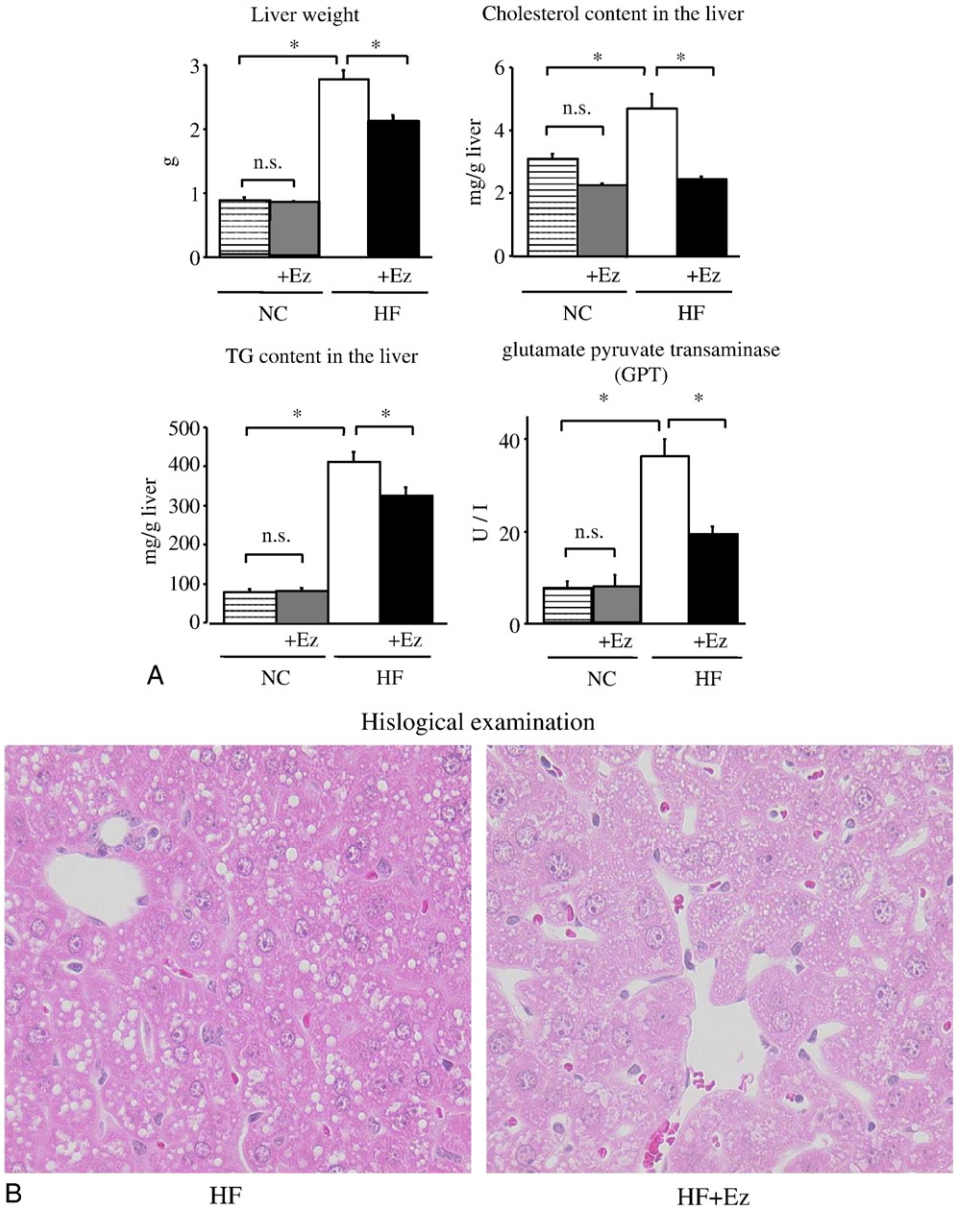

Fig. 2. Impact of ezetimibe on liver steatosis in mice fed a normal chow diet or a high-fat diet. A, Liver weights in the NC, NC + Ez, HF, and HF + Ez groups (n = 9-13). The TG contents (n = 9-10) and cholesterol contents (n = 5) in the livers of the NC, NC + Ez, HF, and HF + Ez groups are shown. The GPT levels in the NC, NC + Ez, HF, and HF + Ez groups are also shown (n = 9-13). B, Histologic analysis of liver samples stained with hematoxylin and eosin (100×) in the HF and HF + Ez groups. The values are the means ± SE. *P < .05.

ezetimibe had no impact on body weight or fat mass in mice fed either a high-fat diet or a normal chow diet (Fig. 1A).

3.2. Impact of ezetimibe on lipid metabolism in mice fed a normal chow or high-fat diet

A high-fat diet significantly increased the serum LDL cholesterol level, but not the TG level (data not shown). Among animals fed a high-fat diet, the addition of ezetimibe significantly lowered the serum cholesterol in the very low-density lipoprotein (VLDL) and LDL fractions, and TG in the VLDL fraction (Fig. 1B, C). The reduction in the cholesterol content was prominent in the VLDL and LDL fractions, especially for smaller-sized particles corresponding to small dense LDL (Fig. 1D). The reduction in the TG content was also prominent in the VLDL and LDL fractions, especially for larger-sized particles corresponding to VLDL1 (Fig. 1E). By contrast, the total cholesterol, LDL cholesterol, and TG levels were unchanged between the NC and NC + Ez groups (data not shown).

3.3. Impact of ezetimibe on liver steatosis in mice fed a normal chow or high-fat diet

A high-fat diet significantly increased the liver weight, the TG content in the liver, the cholesterol content in the liver, and the glutamate pyruvate transaminase (GPT) level. Among animals fed a high-fat diet, ezetimibe significantly lowered the liver weight, the TG content in the liver, and the cholesterol content in the liver, although no significant effects on body weight or visceral fat accumulation were observed (Fig. 2A). Histologic examination revealed that ezetimibe improved high-fat-diet–induced lipid accumulation in the liver (Fig. 2B). In contrast, the liver weights, GPT levels, and hepatic TG contents were unchanged between the NC and NC + Ez groups.

3.4. Impact of ezetimibe on glucose tolerance and insulin sensitivity in mice fed a normal chow or high-fat diet

A high-fat diet significantly increased the fasting plasma glucose level. Ezetimibe had no impact on the fasting plasma glucose level of mice fed either a high-fat diet or a normal chow diet. Of note, ezetimibe significantly strengthened the hypoglycemic effect of insulin in animals fed a high-fat diet, whereas it did not affect insulin sensitivity in animals fed a normal chow diet (Fig. 3A). We next performed a glucose tolerance test. A high-fat diet exacerbated glucose tolerance, compared with a normal chow diet. Under our experimental conditions, ezetimibe had no impact on fasting and postprandial glucose levels in mice fed either a high-fat diet or a normal chow diet but reduced the serum insulin levels after glucose loading in animals fed a high-fat diet (Fig. 3B). This result was consistent with the increase in insulin sensitivity caused by ezetimibe in animals fed a high-fat diet. A hyperinsulinemic-euglycemic clamp study revealed that the administration of ezetimibe improved the GIR and EGP in the liver but did not improve peripheral insulin sensitivity (Fig. 3C). Because hyperinsulinemic-euglycemic clamp studies have been used to investigate insulin-suppressive effect on hepatic glucose production under hyperinsulinemic conditions [24], our results (Fig. 3C) suggest that ezetimibe reverses hepatic insulin resistance under hyperinsulinemic conditions rather than under basal conditions (low concentration of insulin).

To confirm the increased insulin action in mice treated with ezetimibe, we injected insulin into the inferior vena cava and examined insulin-stimulated IRS-1, IRS-2, and Akt phosphorylation. Under basal conditions (low concentration of insulin), phosphorylation of these molecules was indistinguishable between the 2 mouse groups. Ezetimibe significantly enhanced insulin-stimulated Akt phosphorylation and tended to increase insulin-stimulated IRS-2 phosphorylation, although the latter change was not significant (Fig. 3D). Thus, in animals fed a high-fat diet, ezetimibe improved hepatic insulin resistance in association with an increase in IRS-2 and Akt phosphorylation and suppressed hepatic glucose production under hyperinsulinemic conditions.

3.5. Impact of ezetimibe on changes in gene expression profiles in the livers of mice fed a high-fat diet

To identify genes that likely affect glucose and lipid metabolism, we performed a DNA microarray. Of the 45,101 genes examined, 609 were significantly overexpressed and 888 were underexpressed in the livers of the HF + Ez group compared with the livers of the HF group. Interestingly, the lower expression of SREBP-1, ACC, SCD-1, CYP7A1, and liver CPT1 and the higher expression of SREBP2, SHP, HMG-CoA synthase, HMG-CoA reductase, LDL receptor, IRS1, and STAT3 were observed in the livers of the HF + Ez group compared with the livers of the HF group (Table 2). A Taqman PCR analysis confirmed the up-regulation of SREBP-2 and SHP and the down-regulation of SREBP-1c in the livers of the HF + Ez group compared with the livers of the HF group (Fig. 4A, B). The expressions of genes involved in fatty acid β-oxidation and inflammatory reactions were mostly unaltered between the HF and HF + Ez groups, except for the expression of CPT-1 (Table 2). Expression of G6Pase was significantly decreased in the HF + Ez group compared with the HF group, but expressions of glucokinase and PEPCK were unaltered between the 2 groups (Fig. 4C).

Expression of SHP was down-regulated and that of SREBP-1c was up-regulated in the livers on the HF diet compared with those on the normal chow (Fig. 4A).

3.6. No impact of ezetimibe on insulin sensitivity in primary cultured hepatocytes

To examine the ability of ezetimibe to ameliorate hepatic insulin resistance directly in vitro, we established primary cultured hepatocytes and examined insulin-stimulated Akt phosphorylation in the presence of 25 μmol/L of ezetimibe

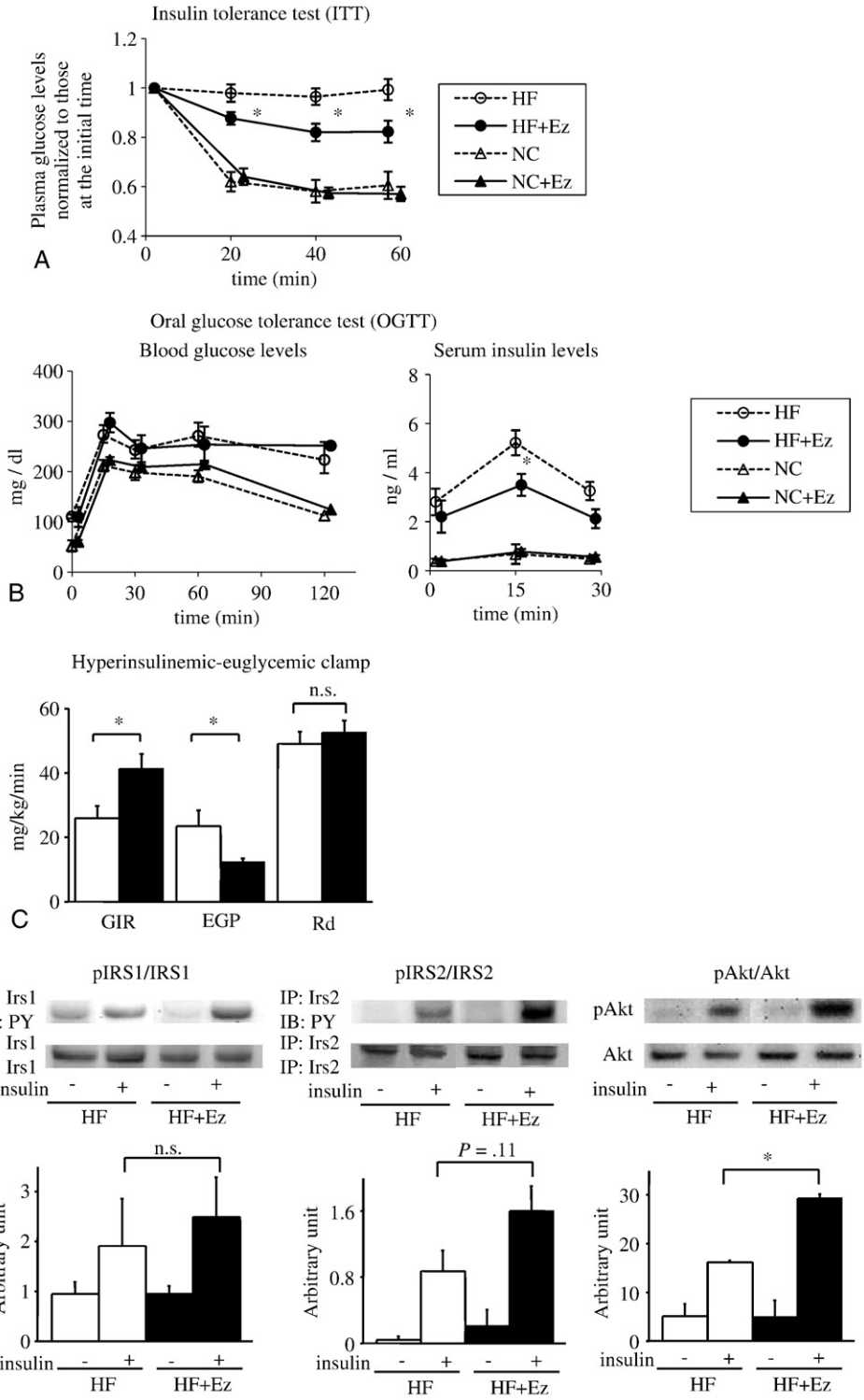

Fig. 3. Impact of ezetimibe on glucose tolerance and insulin sensitivity in mice fed a normal chow or high-fat diet. A, Blood glucose levels during insulin tolerance test in the HF (open circles), HF + Ez (filled circles), NC (open triangles), and NC + Ez (filled triangles) groups (n = 9). B, Blood glucose and plasma insulin levels during an oral glucose tolerance test conducted after 18 hours of fasting in the HF (open circles), HF + Ez (filled circles), NC (open triangles), and NC + Ez (filled triangles) groups (n = 9). C, Glucose infusion rate, EGP, and Rd in the HF (open bar) and HF + Ez (filled bar) groups in a hyperinsulinemic-euglycemic clamp study conducted after 6 hours of fasting (n = 8). D, Insulin-stimulated phosphorylation of Irs1, Irs2, and Akt in the livers of the HF (open bar) and HF + Ez (filled bar) groups (n = 4). The values are the means ± SE. *$P < .05$. HF vs HF + Ez.

Table 2
Changes in gene expression levels in the liver based on a DNA microarray analysis

SREBP pathway		
SREBP1	D	−0.5
SREBP2	I	0.9
Nuclear receptors		
SHP	I	0.5
LXRα, FXR, LRH-1	NS	
Fatty acid and TG biosynthesis		
ACC	D	−0.4
SCD-1	D	−0.5
FAS, ME	NS	
Cholesterol homeostasis and bile acid biosynthesis		
HMG-CoA synthase	I	0.4
HMG-CoA reductase	I	1.4
LDL receptor	I	0.4
CYP7A1	D	−0.9
CYP8B1, ABCA, ABCG5	NS	
Fatty acid β-oxidation		
CPT-1	D	−0.9
MCAD, LCAD	NS	
Insulin signaling		
IRS1	I	0.3
STAT3	I	−1.0
IRS2, CREB, TORC2, CBP, FOXO1, PGC1α	NS	
Inflammatory reactions		
NF-κB, JNK, TNF-α, IKKB, MCP-1, MIP-1α, IL-6	NS	

Log ratios are based on comparisons of HF + Ez vs HF. I indicates increase; D, decrease; NS, no significant change.

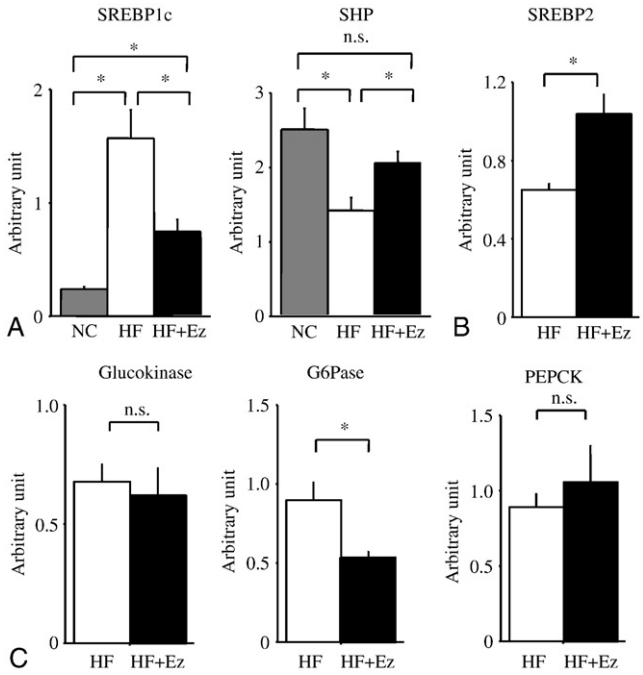

Fig. 4. Impact of ezetimibe on changes in gene expression profiles in the liver. A, Results of Taqman PCR analyses of the expression levels of SREBP-c and SHP in the livers of the NC (gray bar), HF (open bar), and HF + Ez (filled bar) groups (n = 4-6). B, Results of Taqman PCR analyses of the expression levels of SREBP2 in the livers of the HF (open bar) and HF + Ez (filled bar) groups (n = 6). The values are the means ± SE. *$P < .05$. C, Results of Taqman PCR analyses of the expression levels of Gck, G6Pase, and PEPCK in the livers of the HF (open bar) and HF + Ez (filled bar) groups (n = 8-9). The values are the means ± SE. *$P < .05$.

or dimethyl sulfoxide, followed by treatment with 10 nmol/L of insulin. Ezetimibe did not enhance insulin-stimulated Akt phosphorylation in murine cells (Fig. 5), indicating that the improvement in insulin sensitivity induced by ezetimibe in vivo (Fig. 3C, D) cannot be explained by a direct effect on the liver.

3.7. Total bile acid in the serum and liver

The total bile acid concentrations in the serum were very low and indistinguishable among the 4 groups (Fig. 6A). A high-fat diet treatment drastically decreased the total bile acid content in the liver, and ezetimibe significantly increased the total bile acid content in the livers of animals fed a high-fat diet (Fig. 6B).

3.8. RNA interference targeting SHP

To examine the role of SHP in hepatic insulin sensitivity, we performed RNA interference targeting SHP (SHP siRNA). Intravenous injection of siRNA silenced gene expression posttranscriptionally mainly in the liver [25-27] (Fig. 7A). SHP siRNA reduced SHP messenger RNA levels in the liver 24 hours after an injection, but the effects diminished by day 14. SHP siRNA did not significantly affect SREBP-1c expression in the liver under fasting conditions. At day 14, SHP siRNA significantly exacerbated the hypoglycemic effect of insulin in animals fed a high-fat diet (Fig. 7B), whereas it did not affect body weight, fat mass, or liver weight (Fig. 7C). Meanwhile, ezetimibe protected against SHP siRNA-mediated worsening of insulin resistance (Fig. 7B). These results suggest that SHP silencing mainly in the liver worsened insulin resistance and ezetimibe

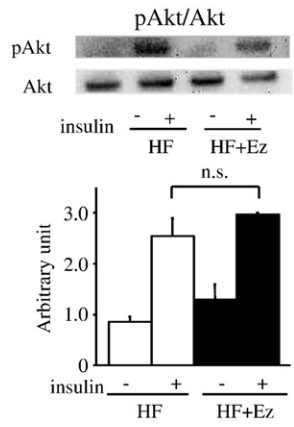

Fig. 5. No impact of ezetimibe on insulin sensitivity in primary cultured hepatocytes. The hepatocytes were incubated with or without ezetimibe (25 μmol/L) for 48 hours, followed by stimulation with insulin (10 nmol/L) for 5 minutes. An immunoblotting analysis was then performed (n = 3). The values are the means ± SE. *$P < .05$.

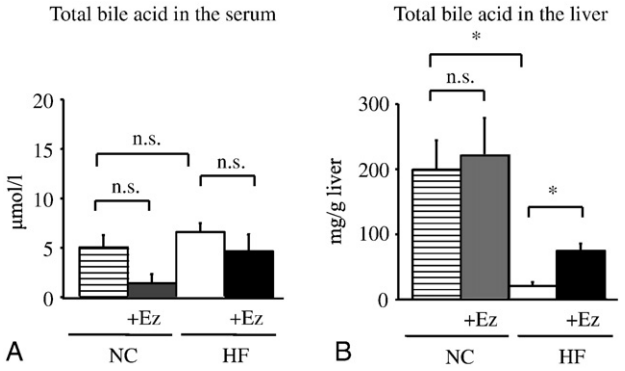

Fig. 6. Total bile acid in the serum and liver. A, Total bile acid levels in the NC, NC + Ez, HF, and HF + Ez groups (n = 5). B, Total bile acid content in the liver of the NC, NC + Ez, HF, and HF + Ez groups (n = 8). The values are the means ± SE. *$P < .05$.

protected mice from insulin resistance associated with the reduction of SHP.

4. Discussion

Previous studies have revealed a potential effect of ezetimibe on insulin sensitivity and glucose metabolism [4,10], but the mechanism responsible for the reversal of insulin resistance has remained unclear. Here, we attempted to reveal the mechanism to explain the effect of ezetimibe on insulin sensitivity and glucose metabolism using C57BL/6 mice with high-fat-diet–induced obesity. We here report 6 findings that link ezetimibe to the reversal of hepatic insulin resistance. First, a euglycemic-hyperinsulinemic clamp study revealed that ezetimibe improved the GIR and EGP in the liver but did not improve peripheral insulin sensitivity (Fig. 3C). Second, ezetimibe improved insulin signaling in the liver, as evidenced by an increase in Akt phosphorylation and a tendency to increase IRS-2 phosphorylation in animals fed a high-fat diet (Fig. 3D). Third, ezetimibe up-regulated SREBP-2 and SHP expression and down-regulated SREBP-1c expression in the liver (Fig. 4). Consistent with these alterations, fatty acid and TG synthesis was suppressed, despite the up-regulation of cholesterol synthesis (Table 2). Fourth, ezetimibe had no impact on insulin sensitivity in primary cultured hepatocytes (Fig. 5). Fifth, a high-fat diet decreased the total bile acid content in the liver; and ezetimibe partially increased it (Fig. 6B). Sixth, SHP silencing mainly in the liver worsened insulin resistance; and ezetimibe protected mice from insulin resistance associated with the reduction of SHP (Fig. 7B). These findings led to our presumption that ezetimibe reverses hepatic insulin resistance via a pathway involving SHP and SREBP-1c in animals fed a high-fat diet.

Unlike rat and human NPC1L1 protein, which is abundantly expressed in the liver, mouse NPC1L1 is predominantly expressed in the intestine [1]. Although it was reported that ezetimibe directly enhanced insulin signaling in HepG2 cells [4], the mechanism seems unlikely to be responsible for the effect of ezetimibe in mice. Thus, NPC1L1 is hardly expressed in murine liver [1]. Consistent with this assumption, ezetimibe had no impact on insulin sensitivity in primary cultured murine hepatocytes (Fig. 5).

Ezetimibe improved insulin signaling in the liver, as evidenced by the increase in Akt phosphorylation, the up-regulation of SHP expression, and the down-regulation of SREBP-1c expressions. What is the molecular link between the up-regulation of SHP, the down-regulation of SREBP-1c, and the reversal of hepatic insulin resistance? The central role of SHP in the process of inhibiting the LXR-SREBP-1c cascade has been reported in studies using SHP knockout mice and pharmacologic experiments [28]. SREBP-1c directly represses the transcription of IRS-2 and inhibits hepatic insulin signaling by inhibiting the downstream PI3K/Akt pathway, leading to a reduction in glycogen synthesis [29]. On the other hand, Yamagata et al [30] reported that bile acids suppress hepatic glucose production in an SHP-dependent fashion, suggesting a potential effect of SHP in the amelioration of insulin resistance via a non–SREBP-1c pathway. This result is consistent with our result that SHP siRNA did not affect SREBP-1c expression in the liver under fasting conditions. However, because expression of SREBP-1c under refed conditions is extremely different from that under fasting conditions [31], further studies are needed to determine whether SHP lowing worsens insulin resistance via SREBP-1c or non–SREBP-1c pathway. Nevertheless, these studies [28-30] support our presumption that ezetimibe reverses hepatic insulin resistance via a pathway involving SHP and SREBP-1c in animals fed a high-fat diet. Furthermore, the presumption is consistent with our result that SHP silencing mainly in the liver worsened insulin resistance and ezetimibe protected mice from SHP-lowing–mediated insulin resistance (Fig. 7B).

It should also be noted that expression of SHP was down-regulated and SREBP-1c was highly up-regulated in the livers of mice fed a high-fat diet compared with the livers of mice fed a normal chow diet. This fact could be one explanation why ezetimibe had no impact on insulin sensitivity in mice fed a normal chow diet, although it reversed hepatic insulin resistance in mice fed a high-fat diet. To sum up, ezetimibe may down-regulate SREBP-1c by up-regulating SHP in the liver and reverses hepatic insulin resistance in mice that have highly expressed SREBP-1c level in the liver.

What is the mechanism for the ezetimibe-induced up-regulation of SHP? SHP is induced in a bile acid–dependent manner in the presence of FXR [32,33] and functions as a direct regulator, consistent with a negative feedback loop in which increased bile acid levels result in a compensatory decrease in the rate of bile acid synthesis [34]. In fact, Watanabe et al [28] demonstrated that bile acids prevent hepatic TG accumulation and VLDL secretion via a pathway involving the up-regulation of SHP and the down-regulation of SREBP-1c in mice fed a high-fat diet. They suggested that

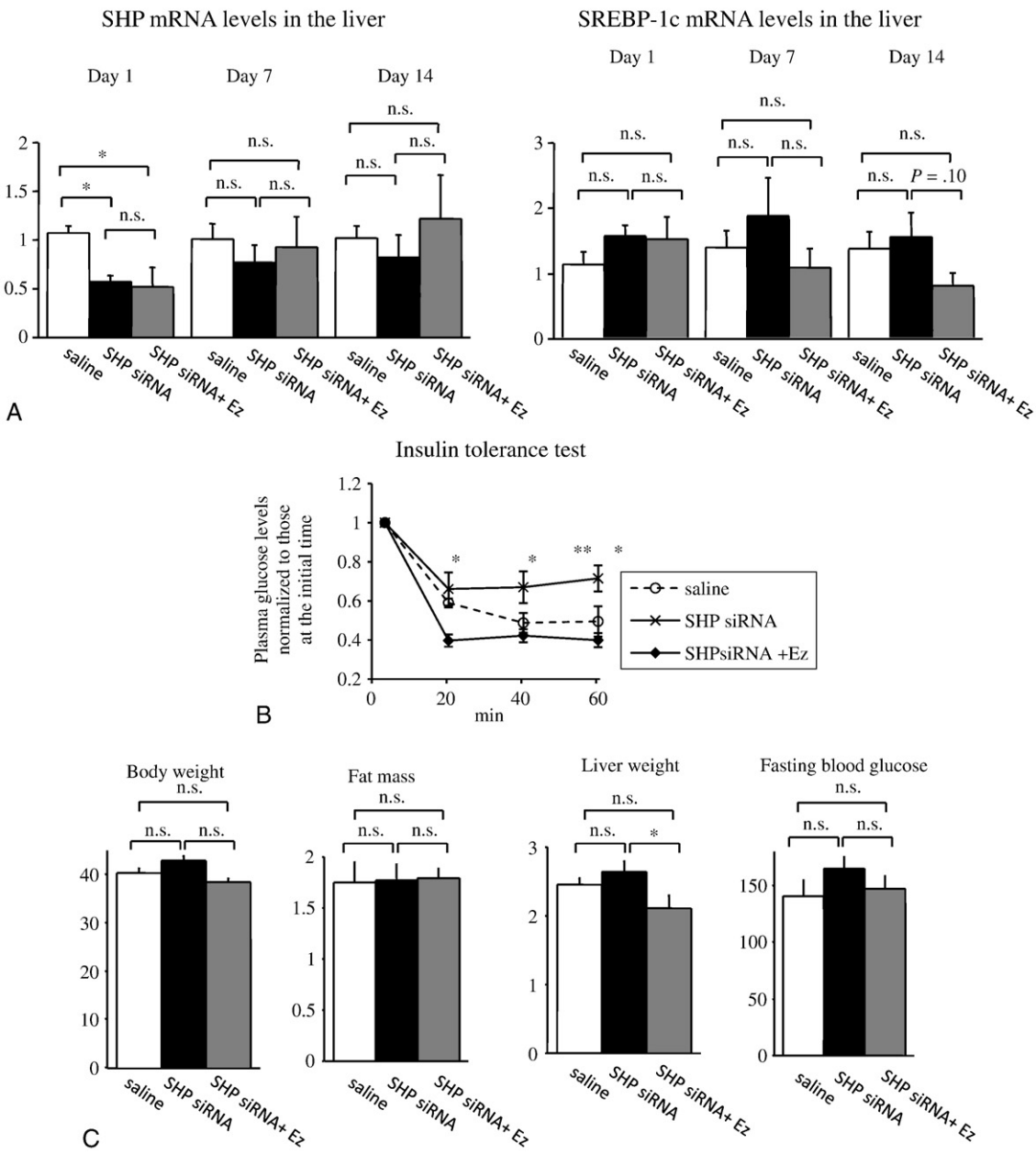

Fig. 7. Impact of intravenous injection of SHP siRNA on body weight, fat mass, liver weight, fasting blood glucose, and insulin sensitivity in mice fed a high-fat diet. A, Results of Taqman PCR analyses of the expression levels of SHP and SREBP-1c in the livers obtained from mice that were injected with saline (open bar), injected with SHP siRNA (filled bar), or treated with ezetimibe after injection of SHP siRNA (gray bar) (n = 3-4). B, Blood glucose levels during insulin tolerance test in mice fed a high-fat diet that were injected with saline (open circle), injected with SHP siRNA (asterisk), or treated with ezetimibe after injection of SHP siRNA (filled square) (n = 4-5). The values are the means ± SE. *$P < .05$ compared with SHP siRNA + Ez. **$P < .05$ compared with saline. C, Body weight, fat mass, liver weight, and fasting blood glucose of mice fed a high-fat diet that were injected with saline (open bar), injected with SHP siRNA (filled bar), or treated with ezetimibe after injection of SHP siRNA (gray bar) (n = 4-5). The values are the means ± SE. *$P < .05$.

a diet-induced increase in the bile acid content in the liver might lead to the up-regulation of SHP. Importantly, ezetimibe increased the total bile acid content in the liver in vivo, despite the down-regulation of CYP7A1 and the absence of any changes in the expressions of CYP8B1, LRH-1, ABCA, or ABCG5 (Table 2). These results suggest that the increased total bile acid content in liver cannot be explained by either an increase in bile acid synthesis or a decrease in the secretion of bile acid in the bile. In fact, it was reported that ezetimibe had no effect on bile acid synthesis in humans or in animal models [3,35,36]. Because the primary effect of ezetimibe is the inhibition of NPC1L1-mediated cholesterol absorption in the intestine, ezetimibe may up-regulate a compensatory uptake of micelle components containing cholesterol, a process that is bile acid dependent but NPC1L1 independent [1,33]. Further research is required

to elucidate how ezetimibe appears to increase the total bile acid content in the liver of C57BL/6 mice fed the types of diets used in the present studies.

What is the relevance of our results to clinical practice in human subjects with insulin resistance? The results of our study indicate that ezetimibe might be effective for ameliorating hepatic insulin resistance under hyperinsulinemic conditions. By contrast, ezetimibe had no substantial impact on insulin sensitivity in animals fed a normal chow diet. This fact suggests that the effectiveness of ezetimibe on improving hepatic insulin sensitivity is dependent on the expression level of SREBP-1c in the liver. Ezetimibe lowered the serum LDL cholesterol level in mice fed a high-fat diet, but failed in mice fed a normal chow diet. The cholesterol content in the normal chow diet was larger than in the high-fat diet (Table 1), but cholesterol absorption can also be affected by body weight and serum cholesterol level itself [37,38]. We therefore assume that high-fat-diet–induced obesity and hypercholesterolemia markedly increased cholesterol absorption in mice fed a high-fat diet and that ezetimibe was more effective under such conditions.

In conclusion, the results of our study support the concept that ezetimibe may ameliorate hepatic insulin resistance as well as dyslipidemia and hepatic steatosis via a pathway involving SHP and SREBP-1c in high-fat-diet–induced obese mice.

Acknowledgment

We are grateful to the Schering-Plough Research Institute for providing us with the ezetimibe used in this study. We thank Mitsuyo Kaji and Eri Sakamoto for their excellent technical assistance and animal care. This work was supported by the Yokohama City University Center of Excellence Program of MEXT and a grant for the Strategic Research Project of Yokohama City University (to YT).

References

[1] Altmann SW, Davis HR, Zhu LJ, Yao X, Hoos LM, Tetzloff G, et al. Niemann-Pick C1 Like 1 protein is critical for intestinal cholesterol absorption. Science 2004;303:1201-4.

[2] Davies JP, Scott C, Oishi K, Liapis A, Ioannou YA. Inactivation of NPC1L1 causes multiple lipid transport defects and protects against diet-induced hypercholesterolemia. J Biol Chem 2005;280:12710-20.

[3] Valasek MA, Repa JJ, Quan G, Dietschy JM, Turley SD. Inhibiting intestinal NPC1L1 activity prevents diet-induced increase in biliary cholesterol in Golden Syrian hamsters. Am J Physiol Gastrointest Liver Physiol 2008;295:813-22.

[4] Deushi M, Nomura M, Kawakami A, Haraguchi M, Ito M, Okazaki M, et al. Ezetimibe improves liver steatosis and insulin resistance in obese rat model of metabolic syndrome. FEBS Lett 2007;581:5664-70.

[5] Labonté ED, Camarota LM, Rojas JC, Jandacek RJ, Gilham DE, Davies JP, et al. Reduced absorption of saturated fatty acids and resistance to diet-induced obesity and diabetes by ezetimibe-treated and Npc1l1−/− mice. Am J Physiol Gastrointest Liver Physiol 2008; 295:776-83.

[6] Assy N, Grozovski M, Bersudsky I, Szvalb S, Hussein O. Effect of insulin-sensitizing agents in combination with ezetimibe, and valsartan in rats with non-alcoholic fatty liver disease. World J Gastroenterol 2006;12:4369-76.

[7] Zheng S, Hoos L, Cook J, Tetzloff G, Davis Jr H, van Heek M, et al. Ezetimibe improves high fat and cholesterol diet-induced non-alcoholic fatty liver disease in mice. Eur J Pharmacol 2008;584: 118-24.

[8] Knopp RH, Dujovne CA, Beaut AL, Lipka LJ, Suresh R, Veltri EP. Evaluation of the efficacy, safety, and tolerability of ezetimibe in primary hypercholesterolaemia: a pooled analysis from two controlled phase III clinical studies. Int J Clin Pract 2003;57:363-8.

[9] Browning JD, Horton JD. Molecular mediators of hepatic steatosis and liver injury. J Clin Invest 2004;114:147-52.

[10] González-Ortiz M, Martínez-Abundis E, Kam-Ramos AM, Hernández-Salazar E, Ramos-Zavala MG. Effect of ezetimibe on insulin sensitivity and lipid profile in obese and dyslipidaemic patients. Cardiovasc Drug Ther 2006;20:143-6.

[11] Davis Jr HR, Compton DS, Hoos L, Tetzloff G. Ezetimibe, a potent cholesterol absorption inhibitor, inhibits the development of atherosclerosis in ApoE knockout mice. Arterioscler Thromb Vasc Biol 2001;21:2032-8.

[12] Folch J, Lees M, Sloane Stanley GH. A simple method for the isolation and purification of total lipids from animal tissues. J Biol Chem 1957;226:497.

[13] Usui S, Hara Y, Hosaki S, Okazaki M. A new on-line dual enzymatic method for simultaneous quantification of cholesterol and triglycerides in lipoproteins by HPLC. J Lipid Res 2002;43:805-14.

[14] Udagawa H, Kitaoka C, Sakamoto T, Kobayashi-Hattori K, Oishi Y, Arai S, et al. Serum cholesterol–decreasing effect of heat-moisture–treated high-amylose cornstarch in cholesterol-loaded rats. Biosci Biotechnol Biochem 2008;72:880-4.

[15] Terauchi Y, Takamoto I, Kubota N, Matsui J, Suzuki R, Komeda K, et al. Glucokinase and IRS-2 are required for compensatory beta cell hyperplasia in response to high-fat diet–induced insulin resistance. J Clin Invest 2007;117:246-57.

[16] Aoki K, Matsui J, Kubota N, Nakajima H, Iwamoto K, Takamoto I, et al. The role of the liver in glucose homeostasis in PI 3-kinase p85α deficient mice. Am J Physiol Endocrinol Metab 2009;296:E842-53.

[17] Kubota N, Terauchi Y, Kubota T, Kumagai H, Itoh S, Satoh H, et al. Pioglitazone ameliorates insulin resistance and diabetes by both adiponectin-dependent and -independent pathways. J Biol Chem 2006;281:8748-55.

[18] Suzuki R, Tobe K, Aoyama M, Inoue A, Sakamoto K, Yamauchi T, et al. Both insulin signaling defects in the liver and obesity contribute to insulin resistance and cause diabetes in Irs2(−/−) mice. J Biol Chem 2004;279:25039-49.

[19] Kubota N, Terauchi Y, Tobe K, Yano W, Suzuki R, Ueki K, Takamoto I, et al. Insulin receptor substrate 2 plays a crucial role in beta cells and the hypothalamus. J Clin Invest 2004;114:917-27.

[20] Berry MN, Friend DS. High-yield preparation of isolated rat liver parenchymal cells: a biochemical and fine structural study. J Cell Biol 1969;43:506-20.

[21] Seglen PO. Incorporation of radioactive amino acids into protein in isolated rat hepatocytes. Biochim Biophys Acta 1976;442:391-404.

[22] Shiroyama K, Moriwaki K, Yuge O. The direct effect of dopamine on glucose release from primary cultured rat hepatocytes. In Vivo 1998;12:527-9.

[23] Zhang G, Budker V, Wolff JA. High levels of foreign gene expression in hepatocytes after tail vein injections of naked plasmid DNA. Hum Gene Ther 1999;10:1735-7.

[24] Bisbis S, Bailbe D, Tormo MA, Picarel-Blanchot F, Derouet M, Simon J, et al. Insulin resistance in the GK rat: decreased receptor number but normal kinase activity in liver. Am J Physiol 1993;265:807-13.

[25] Song E, Lee SK, Wang J, Ince N, Ouyang N, Min J, et al. RNA interference targeting Fas protects mice from fulminant hepatitis. Nat Med 2003;9:226-7.

[26] McCaffrey AP, Meuse L, Pham TT, Conklin DS, Hannon GJ, Kay MA. RNA interference in adult mice. Nature 2002;418:38-9.

[27] Lewis DL, Hagstrom JE, Loomis AG, Wolff JA, Herweijer H. Efficient delivery of siRNA for inhibition of gene expression in postnatal mice. Nat Genet 2002;32:107-8.
[28] Watanabe M, Houten SM, Wang L, Moschetta A, Mangelsdorf DJ, Heyman RA, et al. Bile acids lower triglyceride levels via a pathway involving FXR, SHP, and SREBP-1c. J Clin Invest 2004;113: 1408-18.
[29] Ide T, Shimano H, Yahagi N, Matsuzaka T, Nakakuki M, Yamamoto T, et al. SREBPs suppress IRS-2–mediated insulin signalling in the liver. Nat Cell Biol 2004;6:351-7.
[30] Yamagata K, Daitoku H, Shimamoto Y, Matsuzaki H, Hirota K, Ishida J, et al. Bile acids regulate gluconeogenic gene expression via small heterodimer partner-mediated repression of hepatocyte nuclear factor 4 and Foxo1. J Biol Chem 2004;279:23158-65.
[31] Kamei Y, Miura S, Suganami T, Akaike F, Kanai S, et al. Regulation of SREBP1c gene expression in skeletal muscle: role of retinoid X receptor/liver X receptor and forkhead-O1 transcription factor. Endocrinology 2008;149:2293-305.
[32] Goodwin B, Jones SA, Price RR, Watson MA, McKee DD, Moore LB, et al. A regulatory cascade of the nuclear receptors FXR, SHP-1, and LRH-1 represses bile acid biosynthesis. Mol Cell 2000; 6:517-26.
[33] Lu TT, Makishima M, Repa JJ, Schoonjans K, Kerr TA, Auwerx J, et al. Molecular basis for feedback regulation of bile acid synthesis by nuclear receptors. Mol Cell 2000;6:507-15.
[34] Russell DW, Setchell KD. Bile acid biosynthesis. Biochemistry 1992;31:4737-49.
[35] Repa JJ, Turley SD, Quan G, Dietschy JM. Delineation of molecular changes in intrahepatic cholesterol metabolism resulting from diminished cholesterol absorption. J Lipid Res 2005;46:779-89.
[36] Mathur A, Walker JJ, Al-Azzawi HH, Lu D, Swartz-Basile DA, Nakeeb A, et al. Ezetimibe ameliorates cholecystosteatosis. Surgery 2007;142:228-33.
[37] Mok HY, von Bergmann K, Grundy SM. Effects of continuous and intermittent feeding on biliary lipid outputs in man: application for measurements of intestinal absorption of cholesterol and bile acids. J Lipid Res 1979;20:389-98.
[38] Kesäniemi YA, Miettinen TA. Cholesterol absorption efficiency regulates plasma cholesterol level in the Finnish population. Eur J Clin Invest 1987;17:391-5.